International Journal of Nanoelectronics and Materials
*Volume 13 (Special Issue) Dec 2020* [45-58]

# Adsorption Isotherm Characteristics of Calcium Carbonate Microparticles Obtained from Barred Fish (*Scomberomorus spp.*) Bone Using Two-Parameter Multilayer Adsorption Models

Asep Bayu Dani Nandiyanto[1*], Thyta Medina Salsabila Erlangga[1], Ghina Mufidah[1], Sri Anggraeni[1], Roil Bilad[2] and Jumril Yunas[3]

[1]*Fakultas Pendidikan Matematika dan Ilmu Pengetahuan Alam, Universitas Pendidikan Indonesia, Jl. Dr. Setiabudi No. 229, Bandung 40154, Indonesia.*
[2]*Department of Chemical Engineering, Universiti Teknologi Petronas, Malaysia.*
[3]*Institute of Micro Electronics and Nanotechnology, Universiti Kebangsaan Malaysia, Malaysia.*

**ABSTRACT**

*Adsorption isotherm of calcium carbonate microparticles prepared from calcined barred fish (Scomberomorus spp.) bone at temperature of 600 ℃ was investigated. The experiments were done by testing adsorption ability of the prepared calcium carbonate microparticles (with sizes of 100, 125, and 250* μm*) for adsorbing curcumin molecules (extracted from turmeric) in aqueous solution in the batch-type adsorption reactor. The adsorption results were compared with several two-parameter multilayer adsorption models (i.e. Langmuir, Freundlich, Temkin, Dubinin-Radushkevich, Flory-Huggins, Fowler–Guggenheim, and Hill-de Boer isotherm models). Hill-de Boer model is the best model in this study. The adsorption process takes place on a multilayer surface, and the adsorbent-adsorbate interaction is a physical adsorption (which confirmed and is good agreement with the results from Hill-de Boer models and suitable with Dubinin-Radushkevich, Langmuir, and Temkin models). Adsorption is carried out at different locations energetically under endothermic processes. The Gibbs free energy confirms that the adsorption is spontaneous. The results also confirmed that the smaller adsorbent had a direct impact on the increase in adsorption capacity (due to the large surface area). From all samples, the particle size of 125 μm has a good performance. Particles with smaller size (less than 125 μm) are less optimal in the adsorption process because some aggregation between particles occurs to become larger particles.*

**Keywords:** Adsorption Isotherm, Calcium Carbonate, Fish Bone, Hill-de Boer and Langmuir.

## 1. INTRODUCTION

Calcium carbonate is one of the abundant minerals in nature[1], in which its availability reaches more than 4% in the earth's crust. This material is generally obtained in different polymorphs, such as aragonite, calcite, calcium carbonate monohydrate, calcium carbonate hexahydrate, and vaterite. Calcium carbonate is also the main constituent component in limestone, marble, shells, and coral reefs[2]. Its extraordinary properties allow them for wide applications[3], such as adsorbents, cement, coatings, paper, paints, and copolymers in plastic.

To produce calcium carbonate, many studies have reported several methods, in which they are through carbonation route[4], double decomposition reaction (where they mixed combination of $CaCl_2$ and $Na_2CO_3$; $CaCl_2$ and $(NH_4)_2CO_3$; or $Ca(NO_3)_2$ and $Na_2CO_3$ in solution with equal molar ratios)[5], double charged ion interactions (carbonate and calcium salt as starting material)[6], emulsion and micro emulsion precipitation[7], as well as solution route[8].

*Corresponding Author: *nandiyanto@upi.edu*

Although there have many studies reporting the successful fabrication of calcium carbonate, evaluation of calcium carbonate in the adsorption process is still not much done. In fact, this information is crucial for understanding how the calcium carbonate works in the further development and uses, such as in foods, drugs, and medical-related applications.

This study aimed to investigate and evaluate the adsorption isotherm of calcium carbonate microparticles from barred (*Scomberomorus spp.*) fish bone. Even though many researchers were working on the use of fish bones, transforming them into adsorbent, our novelties are;

i. While other reports typically utilized the process for obtaining hydroxyapatite[9, 10], which are complicated and require multistep processes, our method used a one-step calcination to obtain calcium carbonate. No additional chemical was added during the process since the calcination itself can convert organic components into carbon dioxide and inorganic components into oxide and carbonate.
ii. Most reports discussed the successful synthesis and adsorption process, but less reports presented the adsorption isotherm.
iii. Less reports showed the use of barred fish bone. In fact, barred fish is one of the most product commodities in Indonesia. In 2011, fish commodity from Java Sea in Indonesia reached 861.711 tons, and barred fish reached more than 24.000 tons per year[11]. Barred fish is consumed without bones and the bones were disposed of directly. Different from other organic wastes that can easily decompose and degraded, bones contain calcium carbonate, in which this calcium component is difficult to destroy.
iv. Barred fish bone is attractive since it can be used as a calcium carbonate source alternative[11]. This type of bone is abundant in nature but it is not well used and is found only as an abandoned household waste. Thus, understanding how to create calcium carbonate from barred bone can create further developments and applications in industry.

In the experiment, calcium carbonate was produced only by adding a calcination process for removing organic components; and, to make it microparticles, an additional milling process (as a top down process) was done. The prepared calcium carbonate microparticles were then put into the batch-typed adsorption reactor to analyze the adsorption profile, in which the adsorption results were compared to several two-parameter multilayer adsorption models (i.e. Langmuir, Freundlich, Temkin, Dubinin-Radushkevich, Flory-Huggins, Fowler–Guggenheim, and Hill-de Boer isotherm models).

## 2. MATERIAL AND METHODS

Barred fish (*Scomberomorus spp.*) bone was obtained from the local market in Bandung, Indonesia and used as a calcium carbonate source. The barred fish bone was washed and cleaned to remove dirt and residual meat, soaked in pure water for 15 minutes, dried, and ground using a saw-milling process, in which the saw-milling process was explained in detail in our previous report[12]. The milled fish bones were then put into the calcination using an electrical furnace at 250°C for 2 hours (to convert organic component into carbon, carbon monoxide, and carbon dioxide) and at 600°C for 3 hours (to remove carbon into carbon dioxide and to obtain calcium carbonate).

To obtain particle size distribution, the prepared calcium carbonate powder was put into a sieve test apparatus (PT Rumah Publikasi Indonesia, Indonesia) with various hole sizes of 48, 58, 74, 100, 125, 250, 530, 1000, and 2000 μm) to classify the particle size. The calcium carbonate adsorption test used particles with sizes 100, 125, and 250 μm. To support the analysis, calcium carbonate was characterized using Fourier Transform Infrared (FTIR-4600, Jasco Corp., Japan) and Digital Microscope (BXAW-AX-BC, China).

To evaluate the adsorption of calcium carbonate microparticles, a batch-typed adsorption process was carried out. As a model of adsorbent molecule, curcumin was selected, in which this was obtained by extraction process from Indonesian local turmeric (obtained from Bandung, Indonesia) using the same method as described in our previous reports [13, 14]. The adsorption process was carried out by adding calcium carbonate microparticles to 100 mL of curcumin solution with various concentrations (namely 20, 30, and 50 ppm) at a constant pH, room temperature and pressure conditions, and a stirring condition at 1000 rpm for 20 minutes. After 20 minutes, the solution was filtered to separate the adsorbent from the remaining calcium carbonate particles. Then, the filtrate was analyzed using a Visible Spectroscope (Model 7205; JENWAY; Cole-Parmer; US), analyzed at maximum wavelengths ranging between 280 and 600 nm). The adsorption results were then compared to the standard adsorption isotherm to understand how these adsorption phenomena occurred. Several two-parameter multilayer adsorption models were used, such as Langmuir, Freundlich, Temkin, Dubinin-Radushkevich, Flory-Huggins, Fowler–Guggenheim, and Hill-de Boer isotherm models.

Explanations about the models are described in our previous report[15]. In short, the model equations used in this study are presented in Table 1. In short, the models used the initial concentration of adsorbate ($C_o$; mg/L), the concentration of adsorbate equilibrium ($C_e$; mg/L), and adsorption time ($t$; min). The equations also use the absolute temperature ($T$; K) and the Boltzmann gas constant ($R$; 8.314 J/mol.K). From the equations, several parameters can be obtained:

i. $q_e$ is the amount of molecules adsorbed per gram at equilibrium (mg/g) and $q_m$ is the monolayer adsorption capacity (mg/g).
ii. $K_L$ is the constant in the Langmuir model. $K_F$ is the Freundlich constant as the estimated indicator of adsorption capacity; $A_T$ is the equilibrium constant in the Temkin isotherm model; $K_T$ is the energy constant (L/mg) in Temkin; $\beta$ is the Dubinin-Radushkevich isotherm constant; $K_{FH}$ is the equilibrium Flory-Huggins constant; $K_{FG}$ is the Fowler–Guggenheim equilibrium constant (L/mg); $K_1$ is the Hill–de Boer constant (L/mg)
iii. $R_L$ is the adsorption factor ($R_L > 1$ (the unfavorable adsorption process; $R_L = 1$ (the linear adsorption process; $R_L = 0$ (the irreversible adsorption process); $0 < R_L < 1$ (the favorable adsorption process).
iv. $n$ is the adsorption intensity ($n < 1$ (the chemical adsorption); $n = 1$ (the linear adsorption; $n > 1$ (the physical adsorption); $1 / n < 1$ (the normal adsorption); $1 / n > 1$ (the cooperative adsorption); $1/n$ is near to zero (the heterogenous surface of adsorbent)
v. $B_T$ is the Temkin's isotherm constant ($B_T < 8$ kJ (the physical adsorption); $B_T > 8$ kJ (the chemical adsorption)
vi. $\theta$ is the fraction of adsorbed components on the surface of adsorbent
vii. $\Delta Q$ is the adsorption energy (kJ/mol) and the heat ($\Delta H$; $\Delta H > 0$ kJ/mol is endothermic processes, and $\Delta H < 0$ kJ/mol is the exothermic processes).
viii. $q_s$ is the saturation capacity of theoretical isotherms (mg/g), $\varepsilon$ is the Polanyi potential associated with the equilibrium condition, and $E$ is the energy for predicting type of adsorption ($E$ < 8 kJ/mol (the physical adsorption); $E$ > 8 kJ/mol (the chemical adsorption)
ix. $nFH$ is the number of adsorbate molecules occupying the sorption sites on the surface of adsorbent.
x. $W$ is the interaction energy between adsorbed molecules (kJ/mol) ($W > 0$ kJ/mol (the attraction between adsorbed molecules; the existence of exothermic processes;
xi. $W < 0$ kJ/mol (the repulsion between adsorbed molecules; the existence of endothermic processes); $W = 0$ kJ/mol (no interaction between adsorbed molecules)).
xii. $K_2$ is the energetic constant of the interaction between adsorbed molecules (kJ/mol) ($K_2$ > 0 kJ/mol (the attraction between adsorbed molecules); $K_2 < 0$ kJ/mol (the repulsion

between adsorbed molecules); $K_2$ = 0 kJ/mol (no interaction between adsorbed molecules)).

xiii. $\Delta Gf$ defines the Gibbs energy ($\Delta Gf$ > 0 kJ/mol (the non-spontaneous adsorption); $\Delta Gf$ < 0 kJ/mol (the spontaneous adsorption)).

**Table 1** Isotherm models and their linear form. Table was adopted from reference[15]

| Isotherm model | Initial equation | Linear form | Plot |
|---|---|---|---|
| **Langmuir** | $q_e = \frac{q_m.K_L.C_e}{1+K_L.C_e}$ | $\frac{1}{q_e} = \frac{1}{q_m.K_L}\frac{1}{C_e} + \frac{1}{q_m}$ | $\frac{1}{q_e}$ vs. $\frac{1}{C_e}$ |
| **Freundlich** | $q_e = K_F.C_e^{1/n}$ | $\ln q_e = \ln K_F + \frac{1}{n}\ln C_e$ | $\ln q_e$ vs. $\ln C_e$ |
| **Temkin** | $q_e = B_T(\ln A_T.C_e)$ | $q_e = B_T(\ln C_e) + (B_T \ln A_T)$ | $q_e$ vs. $\ln C_e$ |
| | $\theta = \frac{RT}{\Delta Q}\ln(K_T.C_e)$ | $\theta = \frac{RT}{\Delta Q}\ln(C_e) + \frac{RT}{\Delta Q}\ln(K_T)$ | $\theta$ vs. $\ln(C_e)$ |
| **Dubinin-Radushkevich** | $\ln q_e = \ln q_s - \beta\varepsilon^2$ | $\ln q_e = \ln q_s - \beta\varepsilon^2$ | $\ln q_e$ vs. $\varepsilon^2$ |
| **Flory-Huggins** | $\frac{\theta}{C_O} = K_{FH}(1-\theta)^{nFH}$ | $\ln\left(\frac{\theta}{C_O}\right) = nFH\ln(1-\theta) + \ln K_{FH}$ | $\ln\left(\frac{\theta}{C_O}\right)$ vs. $\ln(1-\theta)$ |
| **Fowler–Guggenheim** | $K_{FG}.C_e = \frac{\theta}{1-\theta}\exp\left(\frac{2.\theta.W}{R.T}\right)$ | $\ln\left(\frac{C_e(1-\theta)}{\theta}\right) = -\ln K_{FG} + \frac{2.\theta.W}{R.T}$ | $\ln\left(\frac{C_e(1-\theta)}{\theta}\right)$ vs. $\theta$ |
| **Hill-de Boer** | $K_1.Ce = \frac{\theta}{1-\theta}\exp\left(\frac{\theta}{1-\theta} - \frac{K_2\theta}{RT}\right)$ | $\ln\left(\frac{C_e(1-\theta)}{\theta}\right) - \frac{\theta}{1-\theta} = -\ln K_1 - \frac{K_2.\theta}{R.T}$ | $\ln\left(\frac{C_e(1-\theta)}{\theta}\right) - \frac{\theta}{1-\theta}$ vs. $\theta$ |

## 3. RESULTS AND DISCUSSION

### 3.1. Physicochemical Properties of Calcium Carbonate Microparticles

Figure 1 (a) shows a typical microscope image of the calcium carbonate microparticles obtained through the carbonation process. Microscope image shows that calcium carbonate microparticles have heterogeneous particle size with some agglomerations.

The result of the sieve test analysis is shown in Figure 1 (b). Calcium carbonate particle sizes were mostly in the range 73 and 1000 μm with mean size particle is 196.41 μm. The most sizes for the calcium carbonate particles are 100, 125, and 250 μm. The main size of calcium carbonate particles is based on the highest percentage of mass distribution of each fraction.

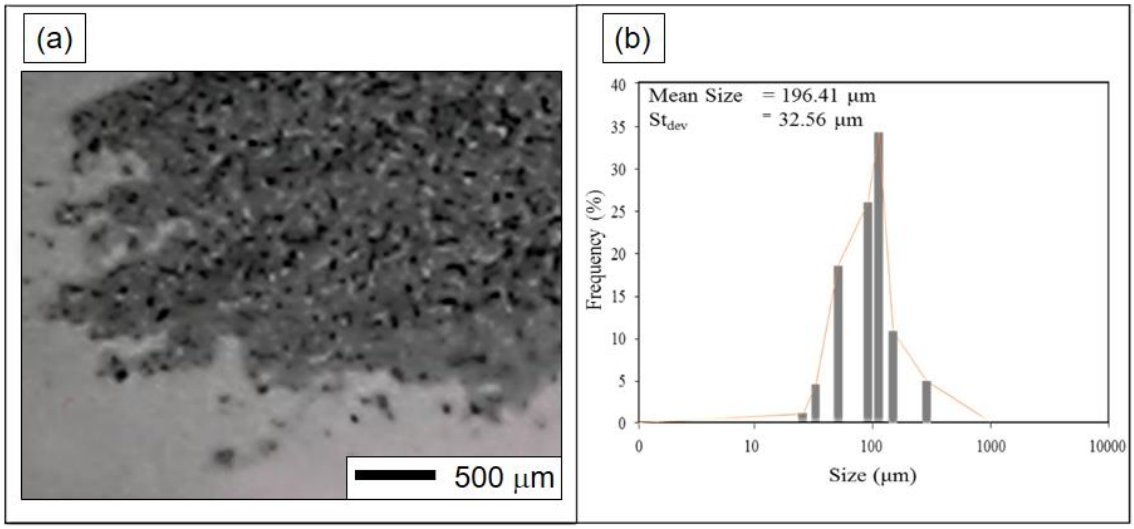


**Figure 1.** Photograph Image of Calcium Carbonate (a) And Particle Size Distribution Based on Sieve Test Measurement (b).

Figure 2 presents the FTIR analysis results. Stretching and bending vibrations of the functional groups were found in the fish bones, fish joints, calcination of fish bones at 250˚C and 600˚C. The FTIR spectra showed that fish bones have calcium carbonate content since found peak at 715, 806, 1086 $cm^{-1}$ which attributed to calcite vibration peak, amine group were recorded at vibration peaks at 1200 – 1700 $cm^{-1}$, and vibration peak at 2875, 2926, and 3310 $cm^{-1}$ shows the vibrations of C-C, C-H, and O-H molecules. It is the same with the fish bone spectra, the fish joints also have vibration peak at 1200 – 1700 $cm^{-1}$ which are indicating amine group and vibration peak at 2875, 2926, and 3310 $cm^{-1}$ shows the vibrations of C-C, C-H, and O-H. However, it does not find vibration peaks at 715, 806, and 1086 $cm^{-1}$ which means it does not contain calcium carbonate. Calcination of fish bones at 250˚C shows no vibration peak of calcium carbonate. This may be due to the removal of all the organic material from the raw material. On the contrary, vibration peaks at 715, 806, 1080 $cm^{-1}$ are indicated as calcium carbonate peaks and all the organic material peaks at 2875 and 2926 $cm^{-1}$ do not observe at higher temperature (600˚C). In this study, thermal stability is important for calcium carbonate formation, where the calcium carbonate can be observed at higher temperature than 250˚C [16, 17].

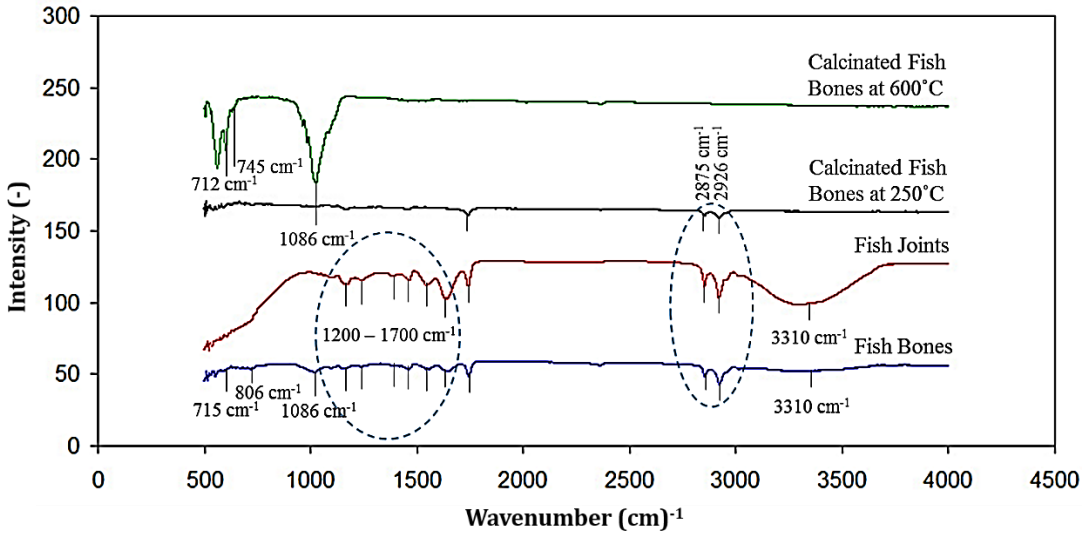


**Figure 2.** FTIR Analysis of Fish Bone and Calcium Carbonate.

### 3.2. Adsorption Analysis Results

The correlation between adsorption efficiency and concentration of adsorbent with various sizes is presented in Figures 3. All data agreed that the efficiency in adsorption of molecules depends on the particle size. The regression results from the data have almost identical gradients, but they have different intercepts. The difference in the intercept value is due to the influence of the surface area on the adsorbent, where the smaller adsorbent, where the smaller adsorbent size has a larger surface area. Then, data were then plotted and compared to various isotherm adsorption models (see Figures 4-10) based on equations presented in Table 1. The plotting data were linearized to get several adsorption parameters, and the adsorption parameters were shown in Table 2.

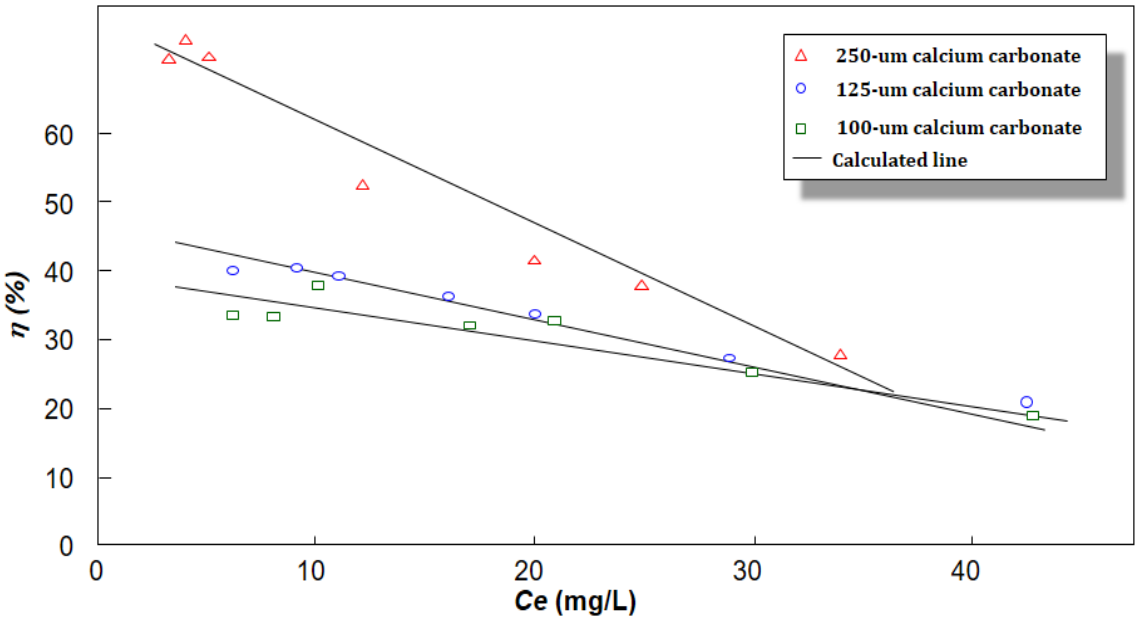


**Figure 3.** Comparison of Experimental and Predicted Efficiency of Adsorption of Calcium Carbonate Microparticles.

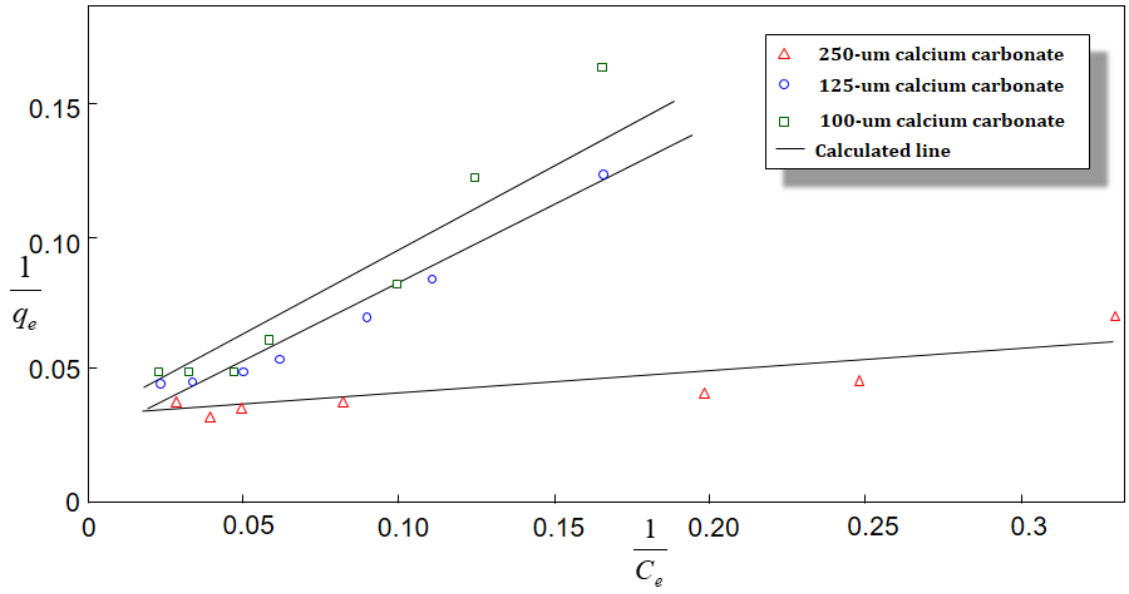


**Figure 4.** Langmuir Isotherm Adsorption of Calcium Carbonate Microparticles.

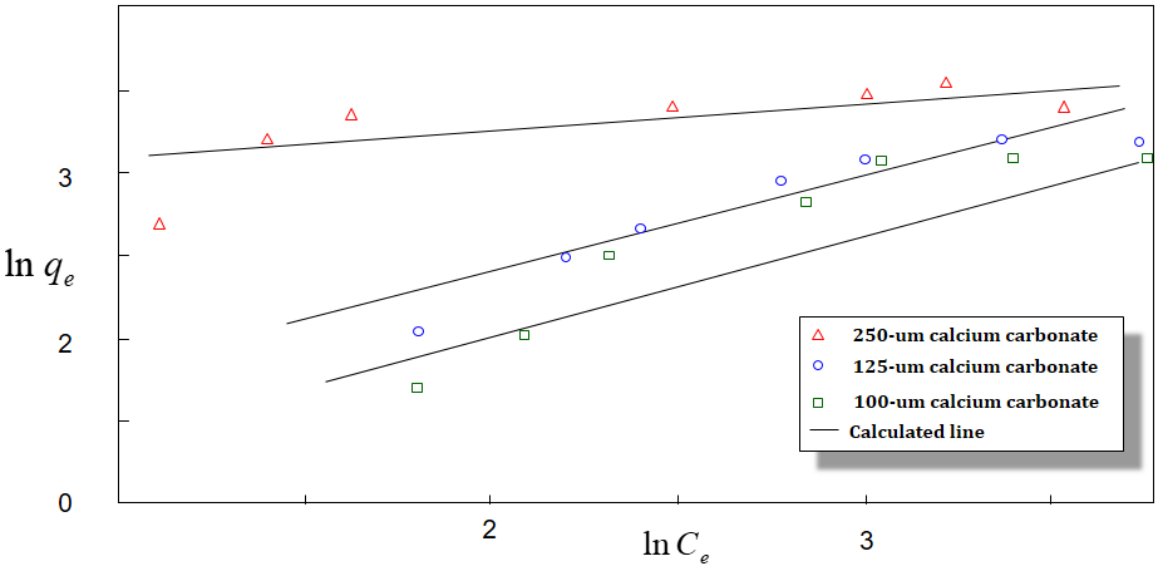


**Figure 5.** Freundlich Isotherm Adsorption of Calcium Carbonate Microparticles.

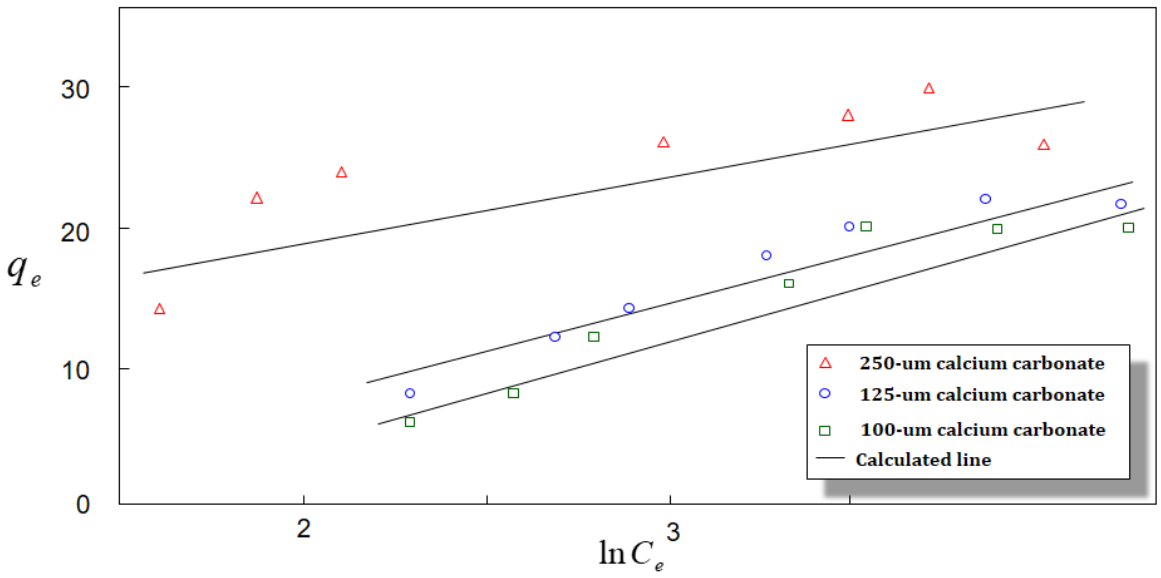


**Figure 6.** Temkin Isotherm Adsorption of Calcium Carbonate Microparticles.

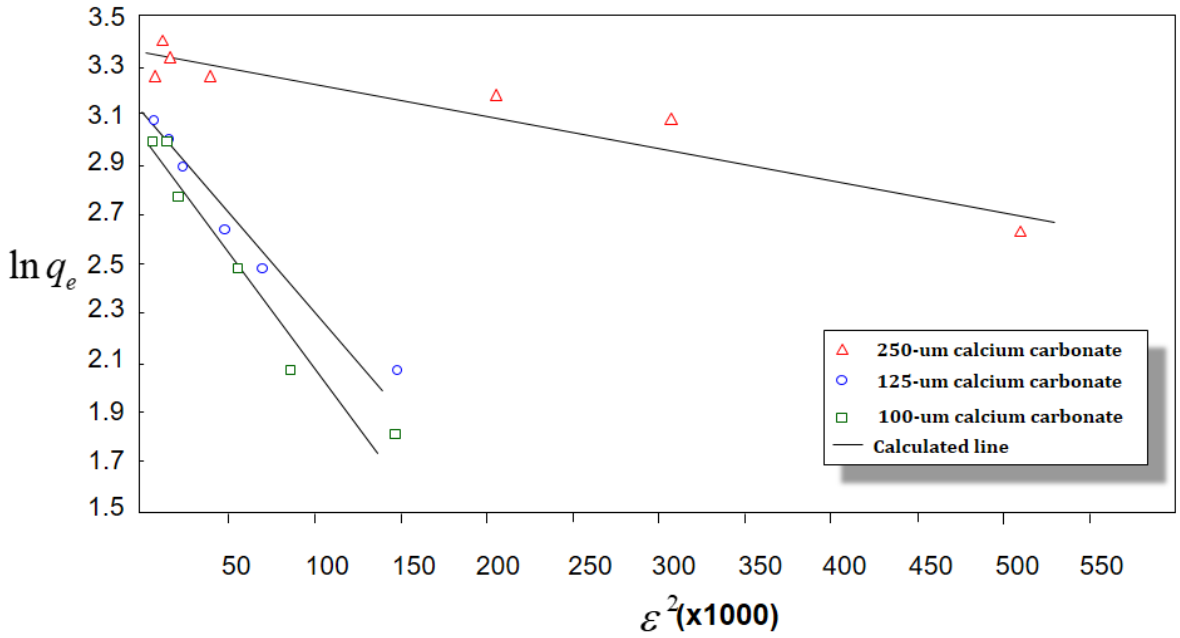


**Figure 7.** Dubinin-Radushkevich Isotherm Adsorption of Calcium Carbonate Microparticles.

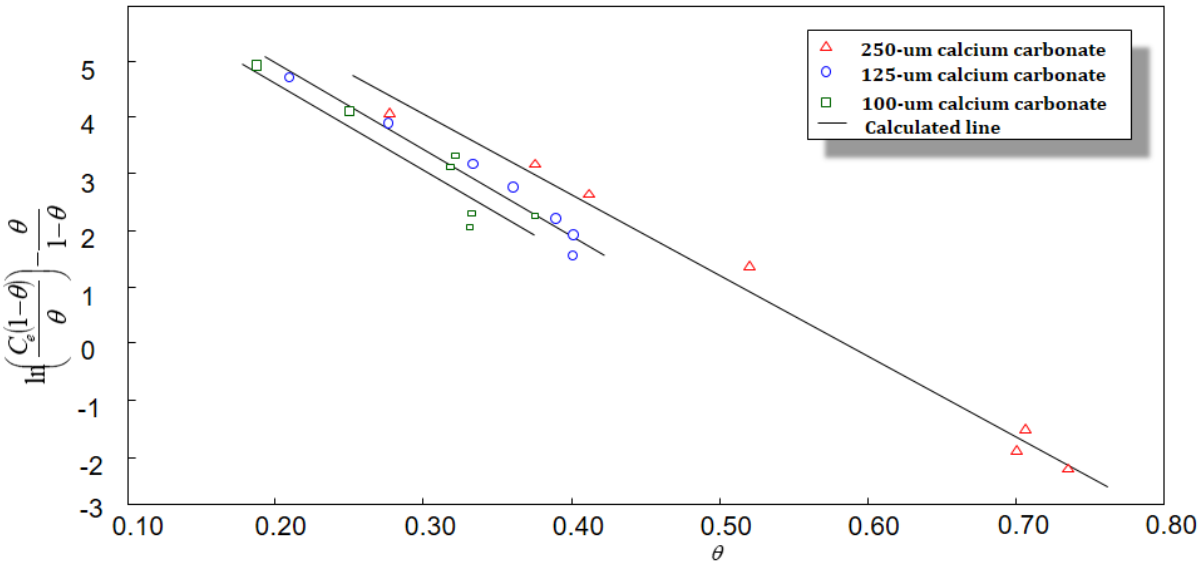


**Figure 8.** Hill-de Boer Isotherm Adsorption of Calcium Carbonate Microparticles.

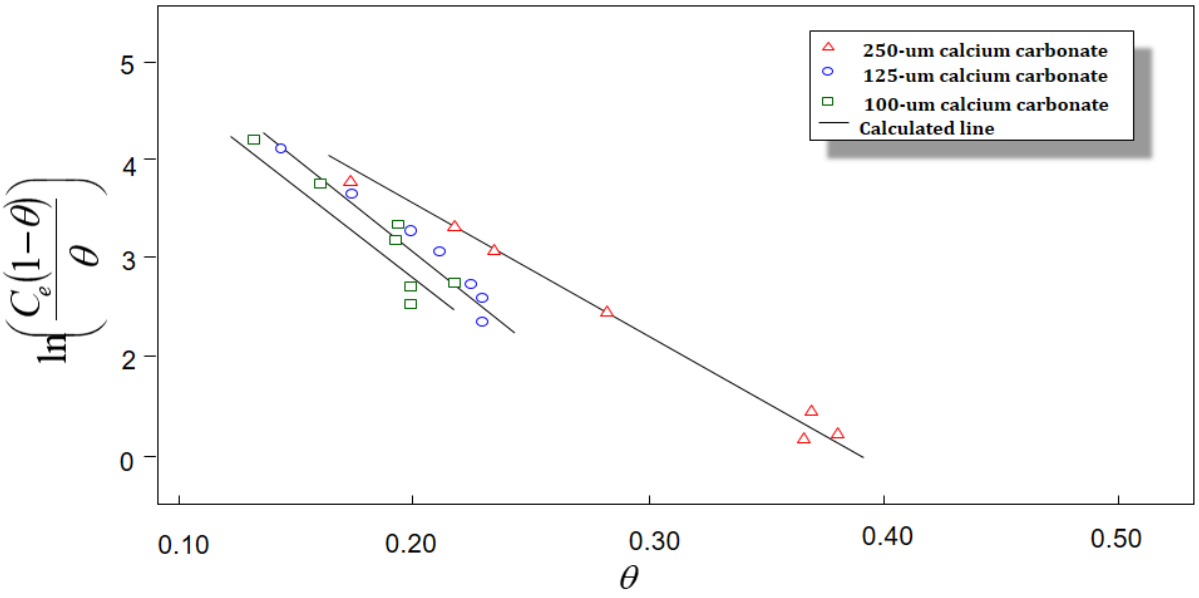


**Figure 9.** Fowler-Guggenheim Isotherm Adsorption of Calcium Carbonate Microparticles.

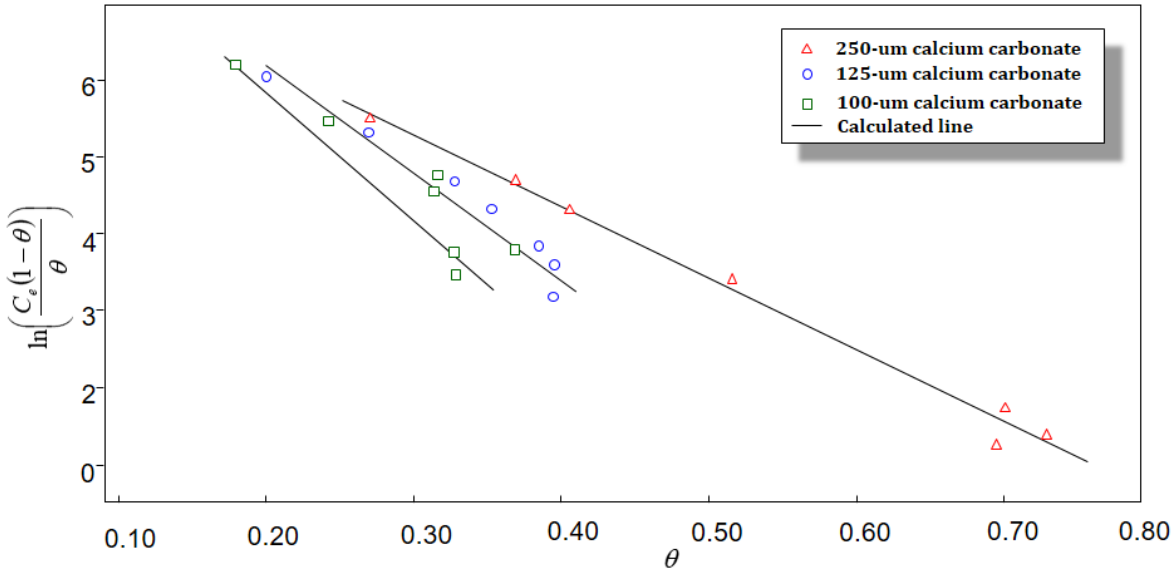


**Figure 10.** Flory-Huggins Isotherm Adsorption of Calcium Carbonate Microparticles.

Based on Figures 4-10 and Table 2, several phenomena happen, depending on the sizes of calcium carbonate microparticles. Explanations are in the following.

For particles of 100 μm, the Langmuir adsorption properties follow a monolayer structure. As shown in Table 2, the $R_L$ value indicates that the process is favorable because the value is 0.2639. The *ΔGf* value also indicates that the process took place spontaneously because the *ΔGf* value is negative. Freundlich's model indicates the approximate adsorption capacity in the physical process (*n* value is more than 1). The adsorption occurs as favorable (with a value of *1/n* = 0.6317) and spontaneous process (expressed by the *ΔGf* value that is less than 0 kJ/mol). The Temkin model shows that adsorption occurs physically (because the $B_T$ value is less than 8 kJ.) and under endothermic condition (the value of *ΔH* is 34.2944 kJ/mol). In the Dubinin-Radushkevic model, the adsorption occurs physically since the *E* value is less than 8 kJ/mol with the *Qs* value of 20.43 mg/g. In the Hill-de Boer model, it was found that the value of the $K_2$ is 41.06 kJ/mol, meaning that there is an interaction between adsorbed molecules. The Fowler – Guggenheim model explains that the existence of repulsion between adsorbed molecules and the negative heat of adsorption (since the value of *W* is -18.13 kJ/mol). The Flory-Huggins model shows the number of molecules adsorbed at the adsorption site on the adsorbent surface, which reaches 8 molecules per adsorption site. The *ΔGf* value is -18.40 kJ/mol., informing that the process occurs spontaneously.

The adsorption properties of 125-μm particles in the Langmuir model follow monolayer structure under favorable process (because the value of $R_L$ = 0.5911). This process is spontaneous with the *ΔGf* value of -39.57 kJ/mol. The Freundlich model indicates the occurrence of chemical adsorption with a value of *1/n* = 0.5204. The process is favorable and occurs spontaneously since the value of the *ΔGf* is less than 0 kJ/mol. In the Temkin model, adsorption occurs physically (because the $B_T$ value is 7.6788 kJ) under endothermic condition (with a *ΔH* value of more than 0 kJ/mol). Based on the experiment results obtained in the Dubinin-Radushkevich adsorption models, the adsorption occurs physically with the *E* value of 0.2618 kJ/mol, and the *Qs* value of 21.63 mg/g. Constant energy interacting with adsorbed molecules in the Hill-de Boer model shows the attraction between adsorbed molecules. The Fowler – Guggenheim model shows that there is a repulsion between adsorbed molecules and negative heat from adsorption, because the resulting *W* value is less than 0 kJ/mol. The Flory-Huggins model shows that seven molecules were adsorbed at the absorption site on the adsorbent surface. In addition, spontaneous absorption also occurred, with a value of *ΔGf* = -18.23 kJ/mol.

The 250-μm particles in the Langmuir model has a monolayer structure and is a favorable because the $R_L$ value is 0.2639. The $\Delta Gf$ value for particles of 250 μm is -34.53 kJ/mol, indicating that this process happens spontaneously. Freundlich's model indicates the occurrence of physical adsorption with a value of $n$ = 4.8608. This process is favorable with a value of $1/n$ = 0.2057 and occurs spontaneously, which is in a good agreement with the 100 and 125 μm. The Temkin model confirmed the $\Delta Gf$ value of 0.205 kJ/mol, the $B_T$ value of 4.4343 kJ, and the $\Delta H$ value of 13.2587 kJ/mol, informing the adsorption occurs physically and endothermic. In the Dubinin-Radushkevich model, the $E$ value of 0.6373 kJ/mol and the $Qs$ value of 28.69 mg/g indicate that adsorption occurs physically. The Hill-de Boer model shows the amount of constant energy of 36.42 kJ/mol, presenting that there is an attraction between adsorbed molecules. The resulting $W$ value in the experiment of -11.66 kJ/mol in the Fowler – Guggenheim Model indicates the presence of repulsion between adsorbed molecules and negative heat in the process. There are two molecules adsorbed at the adsorption site. In the Flory-Huggins model, there is a spontaneous adsorption process because the $\Delta Gf$ value is less than 0 kJ/mol.

Based on the above explanation, the Hill-de Boer model is the best model. In this model, the adsorption process takes place on a multilayer surface and the adsorbent-adsorbate interaction is a physical adsorption (which confirmed and is good agreement with the results from Hill-de Boer models and suitable with Dubinin-Radushkevich, Langmuir, and Temkin models). The results showed that the interaction between the adsorbate and the calcium carbonate surface was carried out multilayer by physical processes[15, 18]. Adsorption is carried out at different locations energetically under endothermic processes. The Gibbs free energy confirms that the adsorption is spontaneous.

The particle size of an adsorbent affects the adsorption performance. The adsorption capacity increases with decreasing particle size. Since adsorption is a surface phenomenon, it correlated to surface area and size of the adsorbents. Surface area has an inverse relationship with particle size[18]. As the surface area of the adsorbent particles increases, the particle size decreases, giving consequences in the increases in adsorption capacity ($Q_{max}$) and saturation capacity per unit mass of the adsorbent increases ($Q_s$). Similarly, in this case, the two samples with small particle sizes (125 and 100 μm) have better adsorption performance than particles having a size of 250 mm (see **Table 2**). By the smaller the particle size of the adsorbent, it means the surface area adsorbent contact with adsorbate is greater. The surface area of a particle is proportional to many pores owned per unit of adsorbent particles. The smaller particle size makes more adsorbate adsorbed. This is caused by small particle size having interagency power bigger molecules thus better absorption.

**Table 2** Adsorption isotherm parameters

| Model | Parameter | Particle size (μm) | | | Notes |
|---|---|---|---|---|---|
| | | 250 | 125 | 100 | |
| **Langmuir** | $Q_{max}$ (mg/g) | 32.91 | 41.23 | 56.57 | The maximum monolayer adsorption capacity |
| | $K_L$ (L/mg) | 0.3264 | 0.0427 | 0.0211 | Langmuir adsorption constant |
| | $R_L$ | 0.2639 | 0.5911 | 0.7331 | $0 < R_L < 1$, favorable adsorption. |
| | $R^2$ | 0.7494 | 0.9681 | 0.9450 | The correlation coefficient. |
| | $\Delta Gf$ (kJ/mol) | -34.53 | -39.57 | -41.31 | $\Delta Gf < 0$, spontaneous process |
| **Freundlich** | $n$ | 4.8608 | 0.5204 | 1.5830 | $n > 1$, adsorption with physical process. |
| | $1/n$ | 0.2057 | 0.5204 | 0.6317 | $1/n = 0 - 1$, favorable adsorption. |
| | $k_f$(mg/g) | 14.6692 | 3.7479 | 2.3492 | The Freundlich constant |

| | | | | | |
|---|---|---|---|---|---|
| | $R^2$ | 0.6199 | 0.8864 | 0.8637 | The correlation coefficient. |
| | $\Delta Gf$ (kJ/mol) | -25.10 | -28.48 | -29.64 | $\Delta Gf$< 0, spontaneous process |
| **Temkin** | $A_T$ (L/g) | 23.2274 | 0.5525 | 0.4077 | The equilibrium binding constant |
| | $B_T$ (J/mol) | 4.4343 | 7.6788 | 7.8867 | $B_T$ < 8 kJ, physical adsorption |
| | $R^2$ | 0.6755 | 0.9386 | 0.9046 | The correlation coefficient. |
| | $KT$ | 0.0056 | 0.0023 | 0.0010 | The Temkin Constant |
| | $\Delta Gf$ (kJ/mol) | 13.2587 | 24.4692 | 34.2944 | $\Delta Gf$ > 0, endothermic process |
| | $R^2$ | 0.9635 | 0.8923 | 0.6881 | The correlation coefficient |
| **Dubinin-Radushkevich** | $Q_s$ (mg/g) | 28.69 | 21.63 | 20.43 | The maximum adsorption capacity of adsorbent. |
| | $\beta$ (mol²/kJ²) | 1.23 | 7.30 | 9.10 | The Dubinin-Radushkevich isotherm saturation capacity |
| | $E$ (kJ/mol) | 0.6373 | 0.2618 | 0.2344 | $E$ < 8 kJ/mol, physical adsorption |
| | $R^2$ | 0.8951 | 0.9644 | 0.9632 | The correlation coefficient |
| **Hill-de Boer** | $K_1$ (L/mg) | 0.000195 | 0.000265 | 0.000281 | Hill–de Boer constant |
| | $K_2$ (kJ/mol) | 36.42 | 38.99 | 41.06 | $K_2$>0, attraction between adsorbed molecules |
| | $R^2$ | 0.9885 | 0.9645 | 0.8705 | The correlation coefficient |
| **Fowler–Guggenheim** | $W$ (kJ/mol) | -11.66 | -16.86 | -18.13 | W < 0, repulsion among adsorbed molecules and negative heat of adsorption |
| | $K_{FG}$ (L/mg) | 0.000749 | 0.000322 | 0.000325 | Fowler–Guggenheim equilibrium constant |
| | $R^2$ | 0.9894 | 0.9565 | 0.8393 | The correlation coefficient |
| **Flory-Huggins** | $nFH$ | 2 | 7 | 8 | Number of adsorbates on the surface site |
| | $K_{FH}$ (L/mg) | 0.003465 | 0.000636 | 0.000596 | Flory-Huggins constant |
| | $\Delta Gf$ (kJ/mol) | -14.04 | -18.23 | -18.40 | $\Delta Gf$< 0, spontaneous process |
| | $R^2$ | 0.9400 | 0.9463 | 0.7702 | The correlation coefficient |

## 4. CONCLUSION

This study has successfully evaluated the adsorption isotherm of calcium carbonate microparticles with sizes of 100, 125, and 250 μm, in which calcium carbonate were obtained from barred fish (*Scomberomorus spp.*) bone. The adsorption results were compared with seven isotherm models (i.e. Langmuir, Freundlich, Temkin, Dubinin-Radushkevich, Flory-Huggins, Fowler-Guggenheim, and Hill-de Boer isotherm models). The analysis showed that the Hill-de boer isotherm presents the best correlation. Based on data of Hill-de Boer models, the adsorption process takes place on a multilayer surface and the adsorbent-adsorbate interaction is a physical adsorption (which confirmed and is good agreement with the results from Hill-de Boer models and suitable with Dubinin-Radushkevich, Langmuir, and Temkin models). The results showed that the interaction between the adsorbate and the calcium carbonate surface was carried out multilayer by physical processes. Adsorption is carried out at different locations energetically under endothermic processes. The Gibbs free energy confirms that the adsorption is spontaneous. The results also confirmed that the smaller adsorbent had a direct impact on the increase in adsorption capacity (due to the large surface area). This research is useful for the further development of calcium carbonate microparticles from organic waste materials.

**ACKNOWLEDGEMENTS**

This study acknowledged RISTEK DIKTI for Grant-in-aid Penelitian Terapan Unggulan Perguruan Tinggi (PTUPT) and Bangdos Universitas Pendidikan Indonesia.

**REFERENCES**

[1] Yamanaka, S.; Oiso, T.; Kurahashi, Y.; Abe, H.; Hara, K.; Fujimoto, T.; & Kuga, Y. Journal of nanoparticle research **16**, 2 (2014) 2266.
[2] Malkaj, P.; & Dalas, E. Journal of Materials Science: Materials in Medicine **18**, 5 (2007) 871-875.
[3] Qian, K.; Shi, T.; Tang, T.; Zhang, S.; Liu, X.; & Cao, Y. Microchimica Acta **173**, 1-2 (2011) 51-57.
[4] Wang, W.; Wang, G.; Liu, Y.; Zheng, C.; & Zhan, Y. Journal of Materials Chemistry **11**, 6 (2001) 1752-1754.
[5] Wu, G.; Wang, Y.; Zhu, S.; & Wang, J. Powder technology **172**, 2 (2007) 82-88.
[6] Ramasamy, V.; Anand, P.; & Suresh, G. Advanced Powder Technology **29**, 3 (2018) 818-834.
[7] Wang, C.; Zhao, J.; Zhao, X.; Bala, H.; & Wang, Z. Powder Technology **163**, 3 (2006) 134-138.
[8] Chen, Y.; Ji, X.; Zhao, G.; & Wang, X. Powder Technology **200**, 3 (2010) 144-148.
[9] Herawati, R.; & Faisal, M. "Utilization of Hydroxyapatite from Tuna Fish Bone Waste as Adsorbent for Cadmium from Aqueous Solutions." Paper presented at the IOP Conference Series: Materials Science and Engineering, (2020).
[10] Venkatesan, J.; & Kim, S.K. Materials **3**, 10 (2010) 4761-4772.
[11] Kasim, K.; & Triharyuni, S. Jurnal Penelitian Perikanan Indonesia **20**, 4 (2016) 235-242.
[12] Nandiyanto, A. B. D.; Andika, R.; Aziz, M.; & Riza, L.S. Indonesian Journal of Science and Technology **3**, 2 (2018) 82-94.
[13] Nandiyanto, A. B. D.; Wiryani, A.; Rusli, A.; Purnamasari, A.; Abdullah, A.; Widiaty, I.; & Hurriyati, R. IOP Conference Series: Materials Science and Engineering **180**, 1 (2017) 012136.
[14] Nandiyanto, A. B. D.; Sofiani, D.; Permatasari, N.; Sucahya, T. N.; Wiryani, A. S.; Purnamasari, A.; Rusli, A.; & Prima, E. C. Indonesian Journal of Science and Technology **1**, 2 (2016) 132-155.
[15] Nandiyanto, A. B. D. Moroccan Journal of Chemistry **8**, 3 (2020) 745-761.
[16] Tizo, M. S.; Blanco, L. A. V.; Cagas, A. C. Q.; Cruz, B. R. B. D.; Encoy, J. C.; Gunting, J. V.; Arazo, R. O.; & Mabayo, V. I. F. Sustainable Environment Research **28**, 6 (2018) 326-332.
[17] Nandiyanto, A. B. D.; Oktiani, R.; & Ragadhita, R. Indonesian Journal of Science and Technology **4**, 1 (2019) 97-118.
[18] Nandiyanto, A. B. D.; Girsang, G. C. S.; Maryanti, R.; Ragadhita, R.; Anggraeni, S.; Fauzi, F. M.; Sakinah, P.; Astuti, A. P.; Usdiyana, D.; & Fiandini, M. Communications in Science and Technology **5**, 1 (2020) 31-39.